



**HAL**  
open science

## Methane and carbon dioxide cycles in lakes of the King George Island, maritime Antarctica

Frederic Thalasso, Armando Sepulveda-Jauregui, Léa Cabrol, Céline Lavergne, Nazlı Olgun, Karla Martinez-Cruz, Polette Aguilar-Muñoz, Natalia Calle, Andrés Mansilla, María Soledad Astorga-España

► **To cite this version:**

Frederic Thalasso, Armando Sepulveda-Jauregui, Léa Cabrol, Céline Lavergne, Nazlı Olgun, et al.. Methane and carbon dioxide cycles in lakes of the King George Island, maritime Antarctica. *Science of the Total Environment*, 2022, 848, 10.1016/j.scitotenv.2022.157485 . hal-04453947

**HAL Id: hal-04453947**

**<https://hal.science/hal-04453947v1>**

Submitted on 18 Apr 2024

**HAL** is a multi-disciplinary open access archive for the deposit and dissemination of scientific research documents, whether they are published or not. The documents may come from teaching and research institutions in France or abroad, or from public or private research centers.

L'archive ouverte pluridisciplinaire **HAL**, est destinée au dépôt et à la diffusion de documents scientifiques de niveau recherche, publiés ou non, émanant des établissements d'enseignement et de recherche français ou étrangers, des laboratoires publics ou privés.

# Methane and carbon dioxide cycles in lakes of the King George Island, maritime Antarctica

Frederic Thalasso <sup>a,b</sup>, Armando Sepulveda-Jauregui <sup>b,c,d</sup>, Léa Cabrol <sup>e,f</sup>, Céline Lavergne <sup>g,h</sup>, Nazlı Olgun <sup>i</sup>, Karla Martinez-Cruz <sup>d,j,k</sup>, Polette Aguilar-Muñoz <sup>g,h</sup>, Natalia Calle <sup>l</sup>, Andrés Mansilla <sup>b,m</sup>, María Soledad Astorga-España <sup>i,\*</sup>

<sup>a</sup> Departamento de Biotecnología y Bioingeniería, Centro de Investigación y de Estudios Avanzados del Instituto Politécnico Nacional (Cinvestav), Av. IPN 2508, Mexico City 07360, Mexico

<sup>b</sup> Cape Horn International Center, Universidad de Magallanes, Av. Bulnes 01855, Punta Arenas 6210427, Chile

<sup>c</sup> Centro de Investigación Gaia Antártica (CIGA), Universidad de Magallanes, Av. Bulnes 01855, Punta Arenas 6210427, Chile

<sup>d</sup> Network for Extreme Environment Research (NEXER), Universidad de Magallanes, Punta Arenas, Av. Bulnes 01855, Punta Arenas 6210427, Chile

<sup>e</sup> Aix Marseille University, CNRS, IRD, Mediterranean Institute of Oceanography (MIO), 163 avenue de Luminy, Marseille 13288, France

<sup>f</sup> Millennium Institute "Biodiversity of Antarctic and Subantarctic Ecosystems" (BASE), Universidad de Chile, Las Palmeras 3425, Nunoa, Santiago de Chile 7800003, Chile

<sup>g</sup> HUB ambiental UPLA and Laboratory of Aquatic Environmental Research (LACER), Centro de Estudios Avanzados, Universidad de Playa Ancha, Subida Leopoldo Carvallo 207, Valparaíso 234000, Chile

<sup>h</sup> Escuela de Ingeniería Bioquímica, Pontificia Universidad Católica Valparaíso, Av. Brasil 2085, Valparaíso 2340000, Chile

<sup>i</sup> Climate and Marine Sciences Division, Eurasia Institute of Earth Sciences, Istanbul Technical University, İTÜ Ayazaga Campus, Maslak, Istanbul 34469, Turkey

<sup>j</sup> Departamento de Ciencias y Recursos Naturales, Universidad de Magallanes, Av. Bulnes 01855, Punta Arenas 6210427, Chile

<sup>k</sup> Environmental Physics, Limnological Institute, University of Konstanz, Mainaustrasse 252, Konstanz 78464, Germany

<sup>l</sup> Departamento de Química, Universidad Técnica Federico Santa María, Av. España 1680, Valparaíso 234000, Chile

<sup>m</sup> Laboratorio de Ecosistemas Marinos antárticos & subantártico, Universidad de Magallanes, Av. Bulnes 01855, Punta Arenas 6210427, Chile

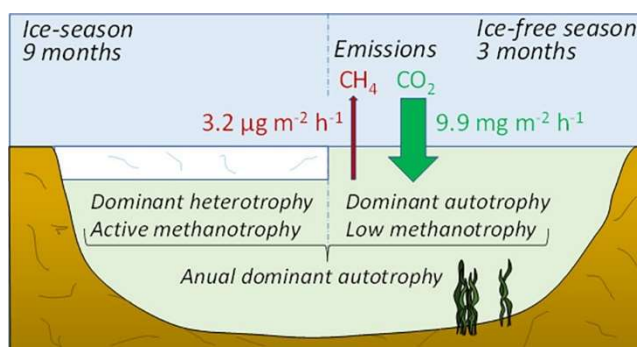
\* Corresponding author at: Av. Bulnes 01890, Punta Arenas 6213029, Chile. E-mail address: msoledad.astorga@umag.cl (M.S. Astorga-España)  
<http://dx.doi.org/10.1016/j.scitotenv.2022.157485>

Received 30 May 2022; Received in revised form 14 July 2022; Accepted 14 July 2022; Available online 20 July 2022

## Science of the Total Environment 848 (2022) 157485

Editor: Jay Gan

### Graphical abstract:



### Highlights:

- CH<sub>4</sub> and CO<sub>2</sub> cycles were characterized in a lake of maritime Antarctica.
- An influx of CO<sub>2</sub> and a low CH<sub>4</sub> efflux were observed during the ice-free season.
- During the ice-season both CH<sub>4</sub> and CO<sub>2</sub> accumulated in the water column.
- Overall, the studied lake acts as a sink of greenhouse gases.
- Similar behavior was observed in 10 other aquatic ecosystems of the region.

### Keywords:

Fluxes  
Dissolved gases  
Greenhouse gas sink/source  
Microbial gene abundance

## ABSTRACT

Freshwater ecosystems are important contributors to the global greenhouse gas budget and a comprehensive assessment of their role in the context of global warming is essential. Despite many reports on freshwater ecosystems, relatively little attention has been given so far to those located in the southern hemisphere and our current knowledge is particularly poor regarding the methane cycle in non-perennially glaciated lakes of the maritime Antarctica. We conducted a high-resolution study of the methane and carbon dioxide cycle in a lake of the Fildes Peninsula, King George Island (Lat. 62°S), and a succinct characterization of 10 additional lakes and ponds of the region. The study, done during the ice-free and the ice-seasons, included methane and carbon dioxide exchanges with the atmosphere (both from water and surrounding soils) and the dissolved concentration of these two gases throughout the water column. This characterization was complemented with an ex-situ analysis of the microbial activities involved in the methane cycle, including methanotrophic and methanogenic activities as well as the methane-related marker gene abundance, in water, sediments and surrounding soils. The results showed that, over an annual cycle, the freshwater ecosystems of the region are dominantly autotrophic and that, despite low but omnipresent atmospheric methane emissions, they act as greenhouse gas sinks.

## Introduction

Freshwater ecosystems cover only about 3.7 % of the Earth's non-glaciated land surface (Verpoorter et al., 2014), but they represent a major methane (CH<sub>4</sub>) and carbon dioxide (CO<sub>2</sub>) source, with an estimated global emission of 1.25–2.30 Pg of CO<sub>2</sub>-equivalents annually, of which CH<sub>4</sub> and CO<sub>2</sub> contribute to 71.8–77.8 % and 19.6–26.1 %, respectively (DelSontro et al., 2018). CH<sub>4</sub> emissions from freshwater ecosystems are the result of two main opposing processes; the anaerobic CH<sub>4</sub> synthesis (methanogenesis) and the aerobic/anaerobic oxidation of CH<sub>4</sub> (methanotrophy; Borrel et al., 2011). On its turn, CO<sub>2</sub> is produced under both aerobic and anaerobic respiration or transported from terrestrial sources (Engel et al., 2018), while it is consumed by CO<sub>2</sub> fixation. CH<sub>4</sub> and CO<sub>2</sub> emissions from freshwater ecosystems have been well described in the literature but most of the numerous reports are on ecosystems located in northern latitudes. For example, the syntheses by Bastviken et al. (2011) and Saunio et al. (2020), both focusing on CH<sub>4</sub>, do not report data emissions from aquatic ecosystems at latitudes below 24°S, while, for CO<sub>2</sub>, data are scarce below 47°S and without any update over the last 10 years (Raymond et al., 2013). The latter brings out the need for a better constrain of CH<sub>4</sub> and CO<sub>2</sub> cycling in southern lakes, to improve the upscaling of global greenhouse gas inventories (Deemer and Holgerson, 2021; Engel et al., 2018).

Lakes in the Antarctic are often subglacial, i.e. perennially ice-covered, and so far about 400 of these have been discovered (Ashmore and Bingham, 2014). In these sealed ecosystems, the CH<sub>4</sub> cycle is active, including methanogenesis (Wand et al., 2006) and oxic CH<sub>4</sub> production (Li et al., 2020), but without any notable exchange with the atmosphere. However, not all Antarctic lakes are subglacial. At the edge of the Antarctic continent, as well as in the peninsula and in the islands surrounding it, i.e. maritime Antarctica, many lakes with a short annual ice-free period, can be found. Contrary to lakes located at other southern latitudes or continental lakes located at similar latitudes in the northern hemisphere, non-perennially glaciated lakes of Antarctica and their surroundings present several characteristics that, all together, make them unique. Indeed, maritime Antarctic

lakes are subject to year-long cold and relatively dry oceanic climate with short mild summers, i.e. cold maritime (Bañón et al., 2013; López-Martínez et al., 2012), and the landscape is characterized by absent or sporadic vegetation, made up of mosses and lichens, resulting in low soil organic content (Burkins et al., 2001; Burkins et al., 2000). Additionally, the water inflow to lakes is mostly limited to precipitations and melted water of snow or glaciers, during the brief mild summer. Thus, these lakes are totally isolated from the atmosphere for 9–11 months per year and have limited exchanges of organic matter with the surrounding environment during the short ice-free period.

The determination of CH<sub>4</sub> cycling in these lakes is of major relevance, not only to fill a knowledge gap but also to contribute establishing the base-line of what is the CH<sub>4</sub> cycle in pristine lakes with low carbon inputs and subject to yearlong cold weather, which are conditions unfavorable to CH<sub>4</sub> production (Beaulieu and Downing, 2019; Martínez-Cruz et al., 2015; Yvon-Durocher et al., 2014).

The determination of CH<sub>4</sub> cycling in these lakes is of major relevance, not only to fill a knowledge gap, but also to contribute establishing the baseline of what is the CH<sub>4</sub> cycle in lakes with low carbon inputs and subject to yearlong cold weather, which are not optimal conditions for CH<sub>4</sub> production (Beaulieu and Downing, 2019; Martínez-Cruz et al., 2015; Yvon-Durocher et al., 2014). Nevertheless, psychrophilic and/or psychrotolerant methanogens have been reported in permanently cold Antarctic environments (Aguilar-Muñoz et al., 2022; Cavicchioli, 2006). Moreover, in the context of climate change, with longer ice-free periods, increased surface temperature and water level (Woolway et al., 2020), and larger ice-free areas in Antarctica (Garbe et al., 2020), these lakes could gain importance and may convert to a standard feature of the future Antarctic landscape. The literature is scarce regarding CH<sub>4</sub> cycling in non-perennially glaciated lakes of Antarctica and only fragmented information is available. Ellis-Evans (1984), found dissolved CH<sub>4</sub> in the water near the sediments, in four lakes of the Signy Island (Lat. 60°S). Sasaki et al. (2010), and Sasaki et al. (2009) have found CH<sub>4</sub> above atmospheric saturation, during the ice-free period, as well as CH<sub>4</sub> bubbles trapped in lake ice during the ice-covered period in freshwater lakes of the Syowa Oasis (Lat. 69°S). Zhu et al. (2010) as well as Ding et al. (2013) have reported summer greenhouse gas emissions from the littoral zone of several freshwater lakes of the Millor peninsula, east Antarctica (Lat. 69°S). More recently, Roldán et al. (2022) have studied the activity and diversity of aerobic methanotrophs in the sediments of the King George Island (Lat. 62°S).

The objective of the present work was to determine the greenhouse gas balance and the dynamic of the CH<sub>4</sub> and CO<sub>2</sub> cycles in non-glacial lakes of the maritime Antarctica, including a high-resolution study of a lake located in the Fildes Peninsula (lake Kitiash; Lat. 62°S), during the ice and the ice-free seasons. Our study included the determination of (i) the dissolved CH<sub>4</sub> and CO<sub>2</sub> concentration in the water column together with several physicochemical parameters, (ii) the CH<sub>4</sub> and CO<sub>2</sub> exchanges with the atmosphere, (iii) the methanotrophic and methanogenic activities in water and sediments, and (iv) the CH<sub>4</sub>-related marker gene abundance in water and sediments. In addition, the possible interactions between lake Kitiash and the surrounding soil environment were investigated. Indeed, the literature indicates that the soil ecosystems surrounding lakes may provide allochthonous carbon inputs, that fuel methanogenesis and carbon mineralization in lakes (Walter et al., 2006; Fuentes et al., 2013). Additionally, the literature also suggests that lateral transport from the littoral zone might be a major source of epilimnetic CH<sub>4</sub> (Peeters et al., 2019). These interactions between lakes and their surroundings have not been established in lakes from maritime Antarctica, characterized by absent or sporadic vegetation, made up of mosses and lichens. Thus, to evaluate how active is the CH<sub>4</sub> cycle in the surrounding soils of the lake, these were characterized in term of CH<sub>4</sub> and CO<sub>2</sub> exchange

with the atmosphere, methanotrophic and methanogenic activities and the CH<sub>4</sub>-related marker gene abundance. Lastly, to seek common features of the CH<sub>4</sub> and CO<sub>2</sub> cycles and their microbial key players in aquatic ecosystems of maritime Antarctica, a partial characterization was also done in 10 additional lakes and ponds of the Fildes Peninsula. This partial characterization included physicochemical characterization, CH<sub>4</sub> and CO<sub>2</sub> fluxes and dissolved concentration, and microbial gene abundance, during the ice-free season.

## **Material and methods**

### **1.1. Study sites and campaigns**

A total of 11 aquatic ecosystems were selected from the Fildes Peninsula of the King George Island (Fig. 1, Table S1A), which were characterized during two field campaigns, at the end of the short summer (i.e. ice-free season) and at the end of the cold season, when all aquatic ecosystems were covered by a thick ice-layer, i.e. ice-season. Among the selected ecosystems, Lake Uruguay (L1), with an area of 7 ha and a maximum depth of 16.5 m was partially characterized over the two seasons. Lake Kitiash (L2) was selected for a high-resolution study, over the two seasons. Lake Kitiash, located at the center of the peninsula, is the largest lake of the region, with an area of 9.4 ha and a maximum depth of 11.0 m. Four other lakes (L3-L6) as well as three ponds (P1-P3), i.e. small and shallow water bodies, were partially characterized during the ice-free season. Lastly, two ponds (OP1, OP2) fully surrounded by moss, that we called “organic ponds”, were also characterized during the ice-free period. Photographs of the selected water bodies are shown on Fig. S1. Except organic ponds, all lakes were surrounded by unsorted soil, composed of mineral and rock fragments as well as volcanic ashes, with absent or scarce colonies of moss and lichens, which is a common feature of the region (Lee et al., 2004). The first campaign took place from February 17th to March 7th 2017 and all ecosystems were ice-free, except OP2 in Ardley Island (with liquid water under a 2-cm thick ice layer). That year, lake Kitiash started to freeze by the beginning of April, thus this campaign corresponded to the end of the ice-free season. The second campaign took place from November 24th to December 12th, 2017. During that campaign, all lakes and ponds were covered by a thick ice-layer, measuring 1.2 m at lake Uruguay and 1.3 m at lake Kitiash. The ice-cover at lake Kitiash melted by mid-January, thus the second campaign can be considered as corresponding to the end of the ice-season.

### **1.2. Physicochemical characterization**

Water depth was measured with a portable sounder (Depthmate Portable Sounder, Speedtech, USA) and the location of each sampling/measurement was determined with a global positioning system (eTrex 20, Garmin, USA). Physicochemical parameters including temperature, pH, dissolved oxygen (DO) concentration, conductivity, and total dissolved solids concentration were measured with a multi-parametric probe (HI 9828, Hanna Instruments, Mexico). These parameters were determined along one depth profile in L1 during the ice-season, along 6 depth profiles in L2 during the ice-season, and along 9 depth profiles in L2 during the ice-free season (Fig. S2). In all cases these profiles were determined from the surface to the sediments at depth intervals of 1 m. Physicochemical parameters were also measured in the other lakes and ponds at the littoral zone and during the ice-free season. Surface water samples were taken at the center of the L2 and at the

littoral zone of the other ecosystems with a 2.2 –L Van Dorn water sampler (Wildco, USA). Nitrate ( $\text{NO}_3^-$ ), ammonium ( $\text{NH}_4^+$ ), nitrite ( $\text{NO}_2^-$ ), and phosphate ( $\text{PO}_4^{3-}$ ) concentrations were measured in duplicate by ion chromatography (ICS-3000, Dionex, Turkey), chlorophyll-a concentration (Chl-a) was determined in triplicate by spectrophotometry using the acetone filter pigment extraction method according to ISO 10260 method (ISO, 1992), while carbonate ( $\text{CO}_3^{2-}$ ) and bicarbonate ( $\text{HCO}_3^-$ ) concentrations were measured in duplicate by titration method. Total Organic Carbon (TOC) and total inorganic carbon (TIC) concentrations were determined in sediment samples, taken at the center of the L2 and at the littoral zone of the other ecosystems. These were analyzed by a TOC/TIC analyzer (TOC-LCPH/CPN, Shimadzu, Turkey). The organic matter content in soil and sediment samples was determined by loss of ignition technique as described in Lavergne et al. (2021).

### 1.3. Dissolved $\text{CH}_4$ and $\text{CO}_2$ concentration

The dissolved  $\text{CH}_4$  ( $C_{\text{CH}_4}$ ) and  $\text{CO}_2$  ( $C_{\text{CO}_2}$ ) concentration in the water column of L1 and L2 during the ice-period were determined using a membrane-integrated cavity output spectrometry method (M-ICOS, Gonzalez-Valencia et al., 2014) coupled to a greenhouse gas analyzer (UGGA, Los Gatos Research, CA, USA). This method allowed for the continuous in situ measurement of dissolved gas at a frequency of  $1 \text{ s}^{-1}$ , which corresponded to approximately 60  $C_{\text{CH}_4}$  and  $C_{\text{CO}_2}$  data per meter of the water column (details provided in the Supporting Information). The lower detection limit of the method under the present configuration was  $80 \text{ ng L}^{-1}$  for  $C_{\text{CH}_4}$  and  $180 \text{ } \mu\text{g L}^{-1}$  for  $C_{\text{CO}_2}$ . During the ice-period, one depth-profile was determined in triplicate at the center of L1, and, 6 depth profiles were determined in triplicates, along a longitudinal East-West transect of L2, after drilling the ice layer with a 10 in. auger (Fig. S2). During the ice-free season, in lake Kitish, where  $C_{\text{CH}_4}$  was below the detection limit of the M-ICOS method, as well as in the other lakes and ponds, a discrete headspace equilibration (HE) technique was used, which allowed to determine  $C_{\text{CH}_4}$  with a detection limit of  $10 \text{ ng L}^{-1}$ . In all lakes/ponds except L2, discrete  $C_{\text{CH}_4}$  was measured in triplicate water samples collected at the surface from the littoral zone. In L2 discrete samples were taken with a Van Dorn sampler, over 9 depth-profiles, along a longitudinal East-West transect (Fig. S2), with 1 m-depth intervals. Briefly, the HE method consisted in transferring the water content of the Van Dorn sampler to 60 mL plastic syringes, ensuring the absence of air bubble. Then, 20 mL of water was gently evacuated and substituted with  $\text{CH}_4$  - and  $\text{CO}_2$  -free nitrogen (99.999 %  $\text{N}_2$ , Linde Gas, Chile). The syringe content was vigorously shaken for 30 s for equilibration, the liquid volume was evacuated, and a 5 mL subsample of the gas content of the syringe was injected into a continuous flow of nitrogen connected to the UGGA in an open circuit. The presence of  $\text{CH}_4$  and  $\text{CO}_2$  in the gas sample was detected as a peak response, that was integrated, after proper calibration with standard  $\text{CH}_4/\text{CO}_2$  samples. Lastly,  $C_{\text{CH}_4}$  and  $C_{\text{CO}_2}$  in the liquid sub-samples were derived from Henry's solubility constant (NIST, 2020).

### 1.4. $\text{CH}_4$ and $\text{CO}_2$ emissions

$\text{CH}_4$  and  $\text{CO}_2$  fluxes were measured from all lakes and from the surrounding soil of L2 during the ice-free season. In all cases, we used a floating chamber method in which the chamber headspace was connected in a loop with the UGGA. For water fluxes, the floating chamber, with an area in contact with water of



0.096 m<sup>2</sup> and a headspace volume of 7.8 L, was gently positioned on the surface of the lake. After 30 s, required to establish stability in CH<sub>4</sub>/CO<sub>2</sub> concentration readings, flux was measured over 3 min. For the determination of fluxes from surrounding soils, a cylindrical PVC chamber with a soil collar and removable PVC lid with airtight rubber seal was used. This chamber, with an area in contact with the soil of 0.041 m<sup>2</sup> and a headspace volume of 12.3 L, was firmly pressed to the ground, and after 5 min, the top of the chamber was closed, and flux measurement was conducted for 5 min. In all cases, flux was determined from the linear slope of CH<sub>4</sub> and CO<sub>2</sub> concentration vs. time in the chamber headspace (Pirk et al., 2016). In L2, water fluxes were determined in triplicates at 31 locations, covering the full lake surface and including the littoral area (Fig. S2). In the other lakes and ponds, fluxes were measured in quintuplicate at one location from the littoral zone, about 1 m from the shore. Around L2, triplicate flux measurements from soils were done at 42 locations, divided in 14 transects of three locations, i.e. at three distances from the shore; as close as possible from the water (< 0.5 m), and at about 3 and 10 m, perpendicularly to the shore (Fig. S2). To confirm the validity of our CH<sub>4</sub> and CO<sub>2</sub> flux measurements at L2, we also combined surface water concentration and wind speeds, to determine flux through the boundary layer method, according to the Kling et al. (1992) method. With that purpose, we used windspeed provided by a nearby station (700 m; Station 950,001, Dirección General De Aeronáutica Civil, 2022).

### **1.5. CH<sub>4</sub> production/oxidation activity in water, sediments and soils**

During both seasons, respirometric assays were performed to determine CH<sub>4</sub> production/oxidation rates in water samples from L2. The method used, described in detail in the Supporting Information, included water sampling at the center of the lake (Fig. S2) along the water column depth, with 2 – m depth intervals, using a Van Dorn sampler. The water samples taken at each depth were transferred to gas-tight glass syringes, and incubated for 5 to 7 days, under dark conditions and at constant temperature. At time intervals, sub-sample were taken and their CH<sub>4</sub> concentration was determined with a headspace equilibration method (described in detail in the Supporting Information). This protocol allowed for the determination of the CH<sub>4</sub> production/oxidation rates without headspace addition, therefore under environmental conditions as close as possible to those prevailing in the lake.

During the ice-free season, the methanogenic potential was determined in surface sediments of L2, P3 and OP2 collected at the center of the ecosystems with an Eckman dredge and in two soil samples surrounding L2 (from East and South transects), with a scoop (0–10 cm layer; approximately 1 kg). The soil samples were taken at one point where no vegetation was observed, and one point where a moss colony was present (soil sample taken under the moss mat; Fig. S2). After the samples were transferred to the laboratory, they were incubated, according to a methodology described in detail in the Supporting Information. Briefly, the samples were first incubated without any amendment, under anaerobic dark conditions at 5 ± 1 °C for 247–330 days. Then, the same samples were split into new vials, spiked with H<sub>2</sub>/CO<sub>2</sub> or acetate, incubated for 50–179 days under the same conditions, to determine the main metabolic route followed by the methanogens.

Methanogenic potential incubations were complemented by methane oxidation potential, i.e. methanotrophic potential rates, in soil samples from L2 (0–10 cm layer; approximately 1 kg), taken during the ice-free season. The samples were collected along four transects (north, south, east, and west shore

of the lake), each transect including three samples collected at three distances from the shore, i.e. same locations where fluxes were determined. Once transferred to the laboratory, the samples were incubated in vials spiked with CH<sub>4</sub>, under dark conditions at 4 ± 1 °C for 10 days during which CH<sub>4</sub> concentration was measured every second day according to [Martinez-Cruz et al. \(2012\)](#). Details are provided in the Supporting Information.

### **1.6. Molecular biology**

During the ice-free season, to assess the main microbial actors involved in the CH<sub>4</sub> cycle, the abundance of specific microbial genes was determined in water and sediments samples of all lakes. The methods used, described in detail in the Supporting Information, included quantitative PCR of bacterial 16S rRNA gene and archaeal 16S rRNA gene as a proxy of bacterial and archaeal abundance, respectively, *mcrA* gene as a proxy of methanogen abundance and *pmoA* gene as a proxy of methane oxidizing bacteria (MOB) abundance.

### **1.7. Data mapping and statistics**

Contour maps of dissolved gases and fluxes were generated by data interpolation according to [Willmott and Matsuura \(2007\)](#), using the mean absolute error (MAE) and the mean bias error (MBE) as criteria using Surfer

11.0 software (Golden Software, USA). Significant differences among data sets (e.g., among lakes, seasons, and water column depths) were tested with a 95 % confidence level. With that purpose, the measured parameters were first tested for normality using the Kolmogorov-Smirnov test. When data were not normally distributed, they were log<sub>10</sub> transformed for comparison purposes. Statistical analyses were done with the NCSS 2000 Statistical Analysis System software (Number Cruncher Statistical Systems, Utah, USA).

In water, soils and sediments, the relationship between CH<sub>4</sub> fluxes and gene markers abundance (*pmoA* and *mcrA*) was evaluated by Spearman correlations (i.e., non-normal distribution tested by the Shapiro test for normality). In peripheral soils of lake Kitiash, the link between the CH<sub>4</sub> emission and CH<sub>4</sub>-related gene abundance was evaluated by an unbalanced (type III) ANOVA using as a factor the dominant CH<sub>4</sub>-related process (i.e. considering “net methanogenesis” in soils with positive CH<sub>4</sub> flux and “net methanotrophy” in soils with negative CH<sub>4</sub> flux). Significant influence of amendment and soil type on methane production rates was determined through ANOVA, normality and homoscedasticity of the residuals were validated by Shapiro and Bartlett tests, respectively. Significant difference between the three amendments was tested by the Tukey's HSD multiple comparison test. These statistical analyses were performed using R software version 4.0.4 ([R Core Team, 2022](#)) in R studio environment version 1.3.959.

## **Results and discussion**

### ***Physicochemical characterization of lake Kitiash (L2)***



A bathymetric map of L2 was built (Fig. S3), showing that the mean depth was 4.5 m and that the maximum depth was 11.5 m (estimated from the interpolated bathymetric map). A relatively extended littoral zone, with depth inferior to 1 m, was observed on the western section of the lake. L2 is characterized by a tributary stream flowing from a small pond and a distributary river that flows to the sea, which is located at approximately 600 m, downstream (Fig. S3). Thus, L2 is an exoreic lake, with an approximately constant volume of  $419 \times 10^3 \text{ m}^3$ , determined from integration of depth data (for the year analyzed).

During the ice-free season, the water column was fully mixed, as evidenced by the absence of temperature gradient (Fig. S4.A). The pH in the water column was also homogeneously distributed and close to neutrality at  $7.23 \pm 0.12$  (mean  $\pm$  one standard deviation of the mean). The water column was fully oxygenated with a DO saturation of  $90.0 \pm 0.8 \%$ . A uniform conductivity of  $119 \pm 0 \mu\text{S cm}^{-1}$  was observed, which corresponded to a salinity of 0.1 PSU, and classifies therefore L2 as a freshwater lake. During the ice-free season, nutrients, alkalinity, and Chl-a concentrations were measured in surface water of L2, while TOC was measured in the sediments (Table S1.B). While the TOC in sediments were relatively high, at 3.16 % dry weight, nutrients and Chl-a classify lake Kitiash as an oligotrophic lake with severe phosphorous limitation (Wetzel, 2001). Regarding nitrates, we measured a concentration of  $0.47 \pm 0.23 \text{ mg L}^{-1}$ . Compared to the literature, the latter is within the large range reported for L2 and other lakes of the King George Island. For instance, Contreras et al. (1991) reported an undetectable level of nitrate in water from lake Kitiash, while Campos et al. (1978) reported nitrate concentrations of tens of  $\text{mg L}^{-1}$  in the same lake. In other lakes, Unrein (2000) reported a range from 0 to  $0.22 \text{ mg L}^{-1}$  in the water of a lake at the southern tip of King George Island, and Neogonekdzarek and Pocięcha (2010) reported a range from 0.15 to  $10.31 \text{ mg L}^{-1}$  in 11 lakes of the King George Island. Thus, nitrates in lakes of the King George Island appears to be highly variable, which might be explained by ornithogenic nutrient input (Sun et al., 2002; Zhu et al., 2009), although Campos et al. (1978) also suggested that nitrates could be due to decomposing mosses at the bottom of the lakes.

During the ice-season, L2 was moderately stratified, as indicated by a gradient of temperature and pH of, respectively,  $1.1 \text{ }^\circ\text{C}$  and 0.83 pH units between surface and bottom water (Fig. S4.A). Similarly, a surface conductivity of  $67 \pm 25 \mu\text{S cm}^{-1}$  was measured at the surface while values of up to  $467 \pm 65 \mu\text{S cm}^{-1}$  were measured at the bottom of the water column (Fig. S5). An additional indicator of stratification during the ice-season was the DO saturation, at  $85.9 \pm 0.9 \%$  in surface water and  $28.9 \pm 22.8 \%$  at the bottom of the water column, in the deeper sections of the lake (Fig. S4.A). The latter is a clear indicator of the existence of active aerobic respiration processes in L2, but certainly low, since the water column was still fully oxygenated despite the absence of exogenous oxygen input during approximately 9 months per year, when the lake was sealed by an ice-cover. The latter may also indicate the presence of active photosynthesis below the ice-cover, as some light was available up to the bottom of the lake, and scarce and irregularly distributed moss colonies were present (see Movie S1), identified as *Drepanocladus polygamus* (Schimp.) Hedenäs (Larraín and Bahamonde, 2017). However, we will show hereafter that under the ice-cover, heterotrophic respiration was dominant over primary production. From the profiles observed during both seasons, L2 might be considered as a monomictic lake, with stratification occurring during the ice-season.

### ***Dissolved CH<sub>4</sub> and CO<sub>2</sub> concentration in lake Kitiesh (L2)***

During the ice-free season, in L2, a first determination of  $C_{CH_4}$  and  $C_{CO_2}$  showed that  $C_{CH_4}$  was below the detection limit of the M-ICOS method. Thus, a HE method was used instead. The results obtained are presented on Fig. S6, showing that due to the mixing of the water column,  $C_{CH_4}$  was homogeneously distributed along the water column. No depth gradient was observed, while relatively higher  $C_{CH_4}$  were found in the eastern and western sections of the lake, compared to the center. Overall,  $C_{CH_4}$  ranged 70.5–86.1 ng L<sup>-1</sup> ( $n = 90$ ), with a mean of  $76.8 \pm 6.0$  ng L<sup>-1</sup>, which is slightly above the atmospheric saturation, determined from the Henry's constant at 63.8 ng L<sup>-1</sup> (NIST, 2020). The measured  $C_{CH_4}$  range is one to two orders of magnitude lower than the  $C_{CH_4}$  reported in freshwater mari-time Antarctic lakes from the Syowa Oasis (Lat. 69°S), by Sasaki et al. (2010). The measured range in L2 is also about 14-fold lower than the  $C_{CH_4}$  found in two Southern Patagonian lakes during spring, which was the season with the lower  $C_{CH_4}$  found over a seasonal study (Gerardo-Nieto et al., 2017). Similarly, surficial water of low nutrient alpine lakes in central Europe (Pighini et al., 2018) have been reported to contain up to three orders of magnitude more dissolved CH<sub>4</sub> concentration than the  $C_{CH_4}$  reported during the ice-free season in L2. During the ice-free season, L2 was characterized by  $C_{CO_2}$  homogeneously distributed with a mean of  $38 \pm 1$  µg L<sup>-1</sup>, which is well below atmospheric saturation (3.3 % of atmospheric saturation estimated to 1.16 mg L<sup>-1</sup>; Fig. S6·B). The latter is a clear indication that during the ice-free season, L2 was dominantly autotrophic, i.e. primary production exceeding heterotrophic respiration, and that it could act as CO<sub>2</sub> sink to the atmosphere due to its moderate alkalinity and basic pH (Cohen and Melack, 2020; Cole and Prairie, 2009, Table S1·B). During the ice-season,  $C_{CH_4}$  and  $C_{CO_2}$  determined with the M-ICOS method in L2, exhibited clear depth gradients (Fig. 2), as well as a significant accumulation, compared to the ice-free season ( $p < 0.05$ ). Indeed, the mean  $C_{CH_4}$  during the ice-season was  $190 \pm 155$  ng L<sup>-1</sup>, which multiplied by the total volume of the lake, corresponded to a total mass of dissolved CH<sub>4</sub> of 79.7 g. The total dissolved CH<sub>4</sub> during the ice-free season was estimated to 32.2 g, thus, a net CH<sub>4</sub> accumulation of 47.5 g (148 %) was observed over 9 months of ice-season. We hypothesize that this CH<sub>4</sub> storage is emitted to the atmosphere shortly after ice break-up, when the winter thermal stratification is lost, and the water column mixes, which is a major CH<sub>4</sub> emission mode in lakes affected by an ice cover during winter (Greene et al., 2014). More dissolved CO<sub>2</sub> was also observed during the ice-season (Fig. 2B), when  $C_{CO_2}$  ranged 0.11–1.04 mg L<sup>-1</sup>, with a mean of  $0.35 \pm 0.20$  mg L<sup>-1</sup>, representing a total mass of 151 kg of CO<sub>2</sub> in the whole lake. Compared to a total mass of 13 kg of CO<sub>2</sub> during the ice-free season, the latter suggests that a net accumulation of 138 kg of CO<sub>2</sub> took place (1050 %) when the lake was covered by an ice layer. Importantly, this CO<sub>2</sub> accumulation within the water column suggests that heterotrophic respiration dominated over primary production, even at the bottom of the water column, where moss colonies were observed (Movie S1). Thus, when covered by an ice layer, the lake, which was dominantly autotrophic during the ice-free season, turned heterotrophic, probably due to the limited amount of light reaching the water column. This is further supported by a significant decrease in DO concentration along depth observed during the ice-season (Fig. S4.A). This seasonal shift from net autotrophy to heterotrophy has been described in boreal lakes (Laas et al., 2012) as well as southern Patagonian lakes (Gerardo-Nieto et al., 2017). It is also important to note that despite CO<sub>2</sub> accumulation

during the ice-season, the final  $C_{CO_2}$  was still below atmospheric saturation (30 % of atmospheric saturation), which is an indication that L2 never reaches saturation and is dominantly autotrophic over the annual cycle. An important corollary of the latter is that the  $CO_2$  that accumulates over the ice-season is not released to the atmosphere but probably metabolized by primary production, after ice break-up and once the water column is fully exposed to sunlight.

### ***CH<sub>4</sub> and CO<sub>2</sub> emissions from lake Kitiash (L2)***

The exchange of  $CH_4$  and  $CO_2$  with the atmosphere were determined during the ice-free season, in L2 and its surrounding terrestrial ecosystem (Fig. 3). As expected from  $C_{CH_4}$  data (slightly above atmospheric equilibrium), positive atmospheric flux (efflux) of  $CH_4$  were observed from L2 surface, ranging 0.618–8.82  $\mu\text{g m}^{-2} \text{h}^{-1}$  with a mean of  $3.21 \pm 1.921 \mu\text{g m}^{-2} \text{h}^{-1}$ . Fluxes, measured through the boundary layer method, were within the same magnitude order, with a range of 0.83–2.76  $\mu\text{g m}^{-2} \text{h}^{-1}$ , and a mean of 1.61  $\mu\text{g m}^{-2} \text{h}^{-1}$ . Regarding the difference between both flux determinations methods, it should be kept in mind that the boundary layer method and chamber measurements were not done on the same day and thus are valid for comparison purposes only. That level of  $CH_4$  emissions is low, compared to other non-perennially glaciated lakes of the Millor Peninsula in Eastern Antarctica, reported by Zhu et al. (2010), i.e. 110–145  $\mu\text{g m}^{-2} \text{h}^{-1}$ , and by Ding et al. (2013), i.e. 40–85  $\mu\text{g m}^{-2} \text{h}^{-1}$ . Our results are closer to those reported by Sasaki et al. (2010) for lakes of the Syowa Oasis, i.e. 13  $\mu\text{g m}^{-2} \text{h}^{-1}$ . Regarding other data collected in southern latitudes, Gerardo-Nieto et al. (2017) reported a total annual emission of 359  $\mu\text{g m}^{-2} \text{h}^{-1}$ , for two lakes in the Southern Patagonia. The  $CH_4$  emission determined during the ice-free season in L2 were also low compared to lakes located at symmetrical latitude in the northern hemisphere. For instance, Bastviken et al. (2011) reported a mean diffusive emission of  $82 \pm 148 \mu\text{g m}^{-2} \text{h}^{-1}$  for northern lakes located at latitude range of 54–66°N. Serikova et al. (2019) also reported  $CH_4$  flux from a large set of Western Siberian lakes (Lat. 62–68°N), where a minimum of 38  $\mu\text{g m}^{-2} \text{h}^{-1}$  was observed. Unambiguously, the climate in these corresponding northern latitudes are significantly different than those found in King George Island, being at boreal latitudes mostly continental, with warm summer. Moreover, northern lakes are commonly characterized by rich surrounding vegetation and ubiquitous permafrost (Obu et al., 2019). In a more global context, the small  $CH_4$  fluxes observed in lake Kitiash were comparable with the three lowest data reported in the global dataset of 227 lakes and 86 reservoirs worldwide analyzed by Deemer and Holgerson (2021). Our data are comparable with  $CH_4$  emissions reported from 7 oligotrophic perialpine and alpine hydropower reservoirs of  $7.4 \pm 6.1 \mu\text{g CH}_4 \text{ m}^{-2} \text{h}^{-1}$  (Diem et al., 2012), and from 16 north temperate lakes ranging between 8 and 36  $\mu\text{g CH}_4 \text{ m}^{-2} \text{h}^{-1}$  depending on their trophic status (West et al., 2016). As expected from the  $C_{CO_2}$  below atmospheric equilibrium in L2, all measurements of  $CO_2$  flux except one, gave negative values, ranging  $-19.2 - 1.2 \text{ mg m}^{-2} \text{h}^{-1}$  with a mean of  $-9.9 \pm 4.3 \text{ mg m}^{-2} \text{h}^{-1}$ . The mean  $CO_2$  flux estimated with the boundary layer method gave fluxes ranging from  $-11.9$  to  $-12.3 \text{ mg m}^{-2} \text{h}^{-1}$ , which is close to the mean flux estimated from chamber measurements and confirms that L2 was a sink of  $CO_2$ . As shown in Fig. 3, the areas with higher  $CO_2$  capture were also the areas with higher  $CH_4$  emission, and a negative correlation between both emissions was observed with a coefficient of correlation ( $R^2$ ) of 0.94 (data not shown). That pattern, i.e. correlation between  $CH_4$  efflux and  $CO_2$  influx, has been reported in other lakes, such as in a mesotrophic lake of Southern Patagonia

(Gerardo-Nieto et al., 2017), and in an oligo- mesotrophic lake in Germany (Martinez-Cruz et al., 2020). We suggest that such pattern is the result of organic matter supplied to the sediments by autochthonous primary productivity and/or transport from littoral zones (Ragg et al., 2021). Assuming that the emissions of CH<sub>4</sub> and CO<sub>2</sub> measured were representative of the entire ice-free season, the total CH<sub>4</sub> emission of the lake was estimated to 648 g year<sup>-1</sup>, while the total CO<sub>2</sub> capture was estimated to 2000 kg year<sup>-1</sup>. When combining CH<sub>4</sub> and CO<sub>2</sub> emissions, in CO<sub>2</sub> equivalent units (CH<sub>4</sub> global warming potential of 34 in a time horizon of 100 years; Myhre et al., 2013), lake Kitiesh was clearly a greenhouse gas sink, with an estimated sink rate of 1978 kg CO<sub>2</sub>-eq year<sup>-1</sup>, and in which the mean annual CH<sub>4</sub> emissions represents 1.10 % of the CO<sub>2</sub> sink.

Over a total of approximately 12 h of continuous chamber deployment in L2, during the ice-free season, no evidence of bubble was observed. In- deed, assuming bubble sizes from 1 to 10 mm (Delsontro et al., 2015) and a CH<sub>4</sub> content in the bubbles of 70 % (Walter Anthony et al., 2010), any bubble reaching the chamber would have generated a step increase in the measured CH<sub>4</sub> concentrations ranging 0.047–47 ppm, easily detectable by the gas analyzer (UGGA). Despite this observation, suggesting that ebullitive flux was not a major emission mode, after drilling the ice layer during the ice-season, occasional bubble inclusions and a few bubbles trains, were clearly observed within the ice layer (Movie S2). Without an analysis of the nature and composition of these trapped bubbles, ebullitive CH<sub>4</sub> emission cannot be confirmed but is certainly plausible, particularly if considering previous observations of bubbles containing CH<sub>4</sub>, trapped in the ice covering lakes in the Syowa Oasis (Sasaki et al., 2009). We therefore acknowledge that the confirmation of ebullitive flux would require longer chamber deployments and/or the use of specific bubble detection methods (Wik et al., 2016).

### ***CH<sub>4</sub> and CO<sub>2</sub> emissions and marker gene abundances from surrounding soils***

In order to establish possible interactions between the lake and its surrounding ecosystem, which was previously suggested by Gregorich et al. (2006) and Elberling et al. (2006) in a lake of the Garwood Valley (78°S), CH<sub>4</sub> and CO<sub>2</sub> emissions to the atmosphere were also determined from soils along the L2 shore (Fig. 3). Over a fringe of 10 m around the lake, negative CH<sub>4</sub> emissions were often but not always observed, suggesting that, contrary to the lake, surrounding soils mainly act as CH<sub>4</sub> sink. Soil CH<sub>4</sub> emissions ranged from -19.50 to 5.02 μg m<sup>-2</sup> h<sup>-1</sup> with a mean of -1.25 ± 4.30 μg m<sup>-2</sup> h<sup>-1</sup>. Abundances of *mcrA* genes in soils with positive CH<sub>4</sub> emissions were significantly different from the *mcrA* gene abundances of soils exhibiting negative CH<sub>4</sub> emissions (type III, unbalanced ANOVA, F = 4.57, *p* < 0.05), positive CH<sub>4</sub> emissions corresponding to higher abundances of *mcrA* gene (on average 2.3 orders of magnitude higher; Table S3). In contrast to the lake, the CO<sub>2</sub> emissions from surrounding soils were dominantly positive, ranging from -14.36 to 35.48 mg m<sup>-2</sup> h<sup>-1</sup> with a mean of 5.43 ± 9.82 mg m<sup>-2</sup> h<sup>-1</sup>. Similarly to what observed by Gregorich et al. (2006), both CH<sub>4</sub> and CO<sub>2</sub> emissions were highly variable at short distance. In some cases, CH<sub>4</sub> and CO<sub>2</sub> fluxes shifted from positive to negative values in a single soil transect, few meters apart. In the same line, we observed high spatial variation of soil microbial biomass quantified by molecular proxies (i.e., gene abundance; Table S3). Even so, CH<sub>4</sub> and CO<sub>2</sub> emissions, as well as microbial gene abundance (bacterial and archaeal 16S rRNA as well as *mcrA* gene abundance) were all significantly correlated with

the organic matter concentration of the soil (Spearman correlation;  $\rho = 0.39, 0.47, 0.47, 0.49$  and  $0.64$ , for bacterial 16S rRNA gene, archaeal 16S rRNA gene and *mcrA* gene, CH<sub>4</sub> and CO<sub>2</sub> emissions, respectively;  $p < 0.05$ ). This confirms the organic matter dependence of biogeochemical processes in poor-C soils (Conrad, 2020). Soil archaea, methanogen and methanotroph abundances were also significantly correlated with soil CO<sub>2</sub> (but not CH<sub>4</sub>) emissions (Spearman correlation;  $\rho = 0.46, 0.42, 0.36$ , for soil archaea, methanogen and methanotroph abundances respectively,  $p < 0.05$ ). However, no correlation was found between aquatic and terrestrial CH<sub>4</sub> or CO<sub>2</sub> emissions, neither with the distance to the shore, nor with the height above the water surface, which prevented reaching any conclusive evidence in regard to the interactions between the lake and the surrounding ecosystem.

### **CH<sub>4</sub> oxidation and production rates and marker gene abundances in water, sediments, and soils**

During both seasons, water samples were taken at several depths of the water column of L2 to determine the methane oxidation/production rates. During the ice-free season, no significant oxidation/production was detected. On the contrary, during the ice-season, a positive CH<sub>4</sub> oxidation was observed, with a mean of  $16.0 \pm 17.3$  ng L<sup>-1</sup> d<sup>-1</sup> and a maximum of  $42.5 \pm 44.5$  ng L<sup>-1</sup> d<sup>-1</sup> at 9 m depth (Fig. 4.A). Two reasons may explain why methanotrophic activity was observed during the ice-cover season, but not during the ice-free season. First, during the ice-free season,  $C_{CH_4}$  was low; i.e. about 70 ng L<sup>-1</sup>. These low concentrations might have been below a threshold concentration value for the methanotrophic process. To this regard, it is worth noting that the CH<sub>4</sub> affinity constant of aerobic methanotrophy has been reported to  $0.11 \pm 0.05$  mg L<sup>-1</sup> (Liikanen et al., 2002; Lofton et al., 2014), i.e. up to 3 orders of magnitude above  $C_{CH_4}$  found in lake Kitiash. The second reason has to do with the detection limit of the method used. Indeed, the incubation method showed an important noise of  $C_{CH_4}$  during incubations, when tested at the lower concentrations, thus preventing the determination of a significant methanotrophic rate. However, it should be noted that, even after 7 days of incubation, CH<sub>4</sub> was still detected in samples incubated from an initial concentration of ca. 70 ng L<sup>-1</sup>, thus we estimated that the methanotrophic rate was in all case  $< 10$  ng L<sup>-1</sup> d<sup>-1</sup>, which can be considered as the method lower limit of detection.

During the ice-season, the abundance of methanogen and methanotroph markers (i.e., *mcrA* and *pmoA* genes, respectively) significantly increased with both water depth (Spearman correlations;  $\rho = 0.86$  and  $0.90$ , respectively;  $p < 0.05$ ) and CH<sub>4</sub> concentrations (Spearman correlations;  $\rho = 0.67$  and  $0.66$ , respectively;  $p < 0.05$ ), while the total abundance of prokaryotes (bacteria and archaea) remained stable over the water column (Fig. 4.B). As the whole water column was oxygenated, it was consistent to retrieve MOB markers until the bottom of the lake, where the maximal *pmoA* abundance ( $1.67 \times 10^8$  copies L<sup>-1</sup> between 8.5 and 9 m depth) was found (representing up to 1.8 % of total prokaryotic abundance). The abundance of *pmoA* gene reached and inclusively outnumbered the abundance found in subalpine stratified lake ( $< 2 \times 10^7$  copies L<sup>-1</sup>; Guggenheim et al., 2019), temperate lakes from Sweden ( $< 7.5 \times 10^6$  copies L<sup>-1</sup>; Samad and Bertilsson, 2017) and subarctic lake ( $< 1.6 \times 10^8$  copies L<sup>-1</sup>; Cabrol et al., 2020). Given that most MOB use CH<sub>4</sub> as sole energy/carbon source, their significant depth-enrichment relative to total biomass is an indication of increasing methane oxidation activity with depth, even though we measured gene abundance and not gene expression.

In the sediments of L2, sampled from the center of the lake during the ice-free season, CH<sub>4</sub> production was not detected in unamended samples (Table S4). However, methanogenic rates of  $0.10 \pm 0.06$   $\mu$ g CH<sub>4</sub> g<sup>-1</sup> dry weight d<sup>-1</sup> were observed in samples spiked with H<sub>2</sub>/CO<sub>2</sub>. Higher methanogenic rates (Tukey's HSD test,  $p < 0.05$ F) were



observed in samples spiked with acetate, reaching a CH<sub>4</sub> production rate of  $0.46 \pm 0.06 \mu\text{g CH}_4 \text{ g}^{-1} \text{ dry weight d}^{-1}$  (Table S4). The absence of detectable CH<sub>4</sub> production in the unamended sediments together with (i) a clear production when substrate was added and (ii) non-negligible levels of *mcrA* gene in the in-situ sediment samples (ranging from  $9.10^2$  to  $2.10^8$  *mcrA* gene copies g DW<sup>-1</sup>, i.e. up to levels comparable to OM-rich sub-Antarctic lake sediments reported by [Lavergne et al., 2021](#); Table S3) suggest a lack of labile substrate in the sediments sampled. To this regard, it should be mentioned, that the sediment sample collected during the ice-free season corresponded to a location where no CH<sub>4</sub> accumulation was observed during the ice-season (red arrow in Fig. S5). In incubations of soils around L2, a clear CH<sub>4</sub> production was systematically found, and methanogenic rates were significantly higher in organic soils compared to inorganic ones (Table S4; Tukey's HSD test,  $p < 0.05$ ). In both types of soils, the methanogenic rates were significantly higher in amended than in unamended samples (Tukey's HSD test,  $p < 0.05$ ), and significant difference was observed between both amendments. Regarding methanotrophy in soils surrounding L2, a clear activity was systematically observed, highly variable and with a mean rate of  $6.4 \pm 6.07 \mu\text{g CH}_4 \text{ g}^{-1} \text{ dry weight d}^{-1}$  (Fig. S7). A comparison between the potential methanotrophic and methanogenic rates in the soils surrounding L2 did not allow to reach conclusive evidence of one process being potentially dominant over the other, both processes being on the same magnitude order ( $\mu\text{g CH}_4 \text{ g}^{-1} \text{ dry weight d}^{-1}$ ). The balance between both processes will therefore depend on the conditions found at short spatial scale in the multiple parameters involved in the CH<sub>4</sub> cycle, which have been shown to be highly variable ([Elberling et al., 2006](#); [Gregorich et al., 2006](#)), but, overall, no clear input of CH<sub>4</sub> from the surrounding soil to the lakes is evidenced.

#### ***CH<sub>4</sub> cycling in other lakes and ponds of the Fildes peninsula and Ardley Island***

During the ice-free season the 10 other lakes and ponds presented similar physicochemical parameters than lake Kitiash, with a mean temperature of  $3.1 \pm 1.9$  °C, DO saturation of  $94.2 \pm 5.8$  %, and a conductivity of  $120 \pm 71$   $\mu\text{S cm}^{-1}$  (Table S1·B). The pH was significantly higher ( $p < 0.05$ ) in all lakes and ponds, compared to lake Kitiash, with a mean value of  $8.40 \pm 0.41$ . Uruguay lake, where a physicochemical profile was determined during the ice-season (Fig. S4·B) exhibited similar profiles than those observed in lake Kitiash, including a relatively strong conductivity gradient probably due to marine influence as previously reported ([Contreras et al., 1991](#); Fig. S5). Thus, all sampled lakes and ponds in the Fildes Peninsula can be considered as freshwater ecosystems, fully oxygenated and with a moderately alkaline pH.

Nitrate concentration in the surface water samples ranged  $0.001$ – $0.21$  mg L<sup>-1</sup> for NO<sub>3</sub><sup>-</sup>, if excluding OP2 with a relatively high concentration of  $3.12$  mg L<sup>-1</sup>. Similarly, NH<sub>4</sub><sup>+</sup> in OP2 was  $1.09$  mg L<sup>-1</sup>, while the range measured in the other ecosystems was  $<0.001$ – $0.18$  mg L<sup>-1</sup>. Nitrite and PO<sub>4</sub><sup>3-</sup> were in all case inferior to the detection limit ( $0.001$  mg L<sup>-1</sup>; Table S1·B). Dissolved bicarbonate (HCO<sub>3</sub><sup>-</sup>) ranged  $15.5$ – $34.5$  mg L<sup>-1</sup>, while no carbonate ion (CO<sub>3</sub><sup>2-</sup>) contributed to the total alkalinity (Table S1·B). Chl-a values of the lakes and ponds ranged  $0.29$ – $1.46$   $\mu\text{g L}^{-1}$  (average  $0.70 \pm 0.44$   $\mu\text{g L}^{-1}$ ), if excluding OP1 and OP2, which exhibited a concentration of  $2.64$  and  $6.92$   $\mu\text{g L}^{-1}$ , respectively. Based on Chl-a, the trophic status of the aquatic ecosystems (excluding OP1 and OP2) ranged from ultra-oligotrophic to oligotrophic. From microscopic examination, it was observed that the phytoplankton of all ecosystems were mostly composed of pennate diatoms. The highest NO<sub>3</sub><sup>-</sup>, NH<sub>4</sub><sup>+</sup>, and Chl-a concentrations were measured in OP2 located in the Ardley Island, which is an Antarctic Specially Protected Area (ASPA 150) with important colonies of Gentoo, Adélie and Chinstrap penguins. Thus, the higher primary productivity in OP2 is most likely caused by ornithogenic nutrient input ([Sun et al., 2002](#); [Zhu et al., 2009](#)). Fildes Peninsula on the other



hand, is less affected by ornithogenic activity and the general lithology was composed of altered basaltic rock outcrops with less moss and lichens when compared to Ardley Island.

Regarding dissolved gases, in the 10 aquatic ecosystems distributed on the Fildes Peninsula,  $C_{CH_4}$  ranged 72.1–506.3 ng L<sup>-1</sup> (Fig. S8), the higher concentration being observed, again, in the organic pond OP2. These  $C_{CH_4}$  were measured during the ice-free season, but OP2 was already covered by an ice layer and is therefore not comparable with the other ice-free ecosystems. Overall, the mean  $C_{CH_4}$  measured in the 10 ecosystems (excluding OP2) was  $186 \pm 130$  ng L<sup>-1</sup>, which is about twice higher to what found during the same season in lake Kitiash but lower than the range of  $C_{CH_4}$  reported by Sasaki et al. (2010), for lakes with salinity <1 PSU, i.e. 310–6144 ng L<sup>-1</sup>. Notably, the magnitude of  $C_{CO_2}$  was higher in all ecosystems compared to Kitiash and four of these ecosystems presented a  $C_{CO_2}$  from 10 to 23 % above saturation (Fig. S8). The ecosystems where  $C_{CO_2}$  above saturation were found were all shallow lakes, while the two relatively deep lakes (L1 and L2) and all ponds and organic ponds were undersaturated in CO<sub>2</sub>.

Overall, the CH<sub>4</sub> emission observed from L2 was higher than those observed from the 5 other lakes and above the mean emission of all ecosystems ( $1.7 \pm 1.9$  μg m<sup>-2</sup> h<sup>-1</sup>; Fig. S9), if excluding an outlier with an unexplained CH<sub>4</sub> emission of  $21.5 \pm 7.8$  μg m<sup>-2</sup> h<sup>-1</sup> (P2). Regarding CO<sub>2</sub> emissions, L2 also presented a higher CO<sub>2</sub> sink rate than the other ecosystems, which presented a mean flux of  $-2.69 \pm 1.94$  mg m<sup>-2</sup> h<sup>-1</sup> (Fig. S9). In these other ecosystems, a positive significant correlation was found between the CO<sub>2</sub> emissions and bacterial abundance in water (bacterial 16S rRNA gene abundance; Spearman correlation;  $\rho = 0.67$ ,  $p < 0.05$ ), which suggests that an increase in microbial biomass was linked to an increased contribution of heterotrophic metabolism. As shown on Fig. S9 and contrastingly to lake Kitiash, three ecosystems presented a positive CO<sub>2</sub> emission, but the mean emission was negative. These results suggest that the aquatic ecosystems of the Fildes Peninsula are dominantly autotrophic, at least during the ice-free season. During the ice-season, in Uruguay lake, the  $C_{CO_2}$  depth profile (Fig. S10) indicated that, in accordance with what observed in lake Kitiash, the water column remained clearly undersaturated. The other ecosystems, shallows, were likely to be fully frozen for most part of the year. Thus, over a year cycle, it can be concluded that the lakes and ponds of the region are dominantly autotrophic and a sink of greenhouse gas.

## Conclusions

The CH<sub>4</sub> cycle in the non-perennially glaciated aquatic ecosystems of the Fildes Peninsula is active, resulting in low but omnipresent atmospheric CH<sub>4</sub> emissions during the brief ice-free season. These CH<sub>4</sub> emissions are compensated by a significant capture of atmospheric CO<sub>2</sub>, making them greenhouse gas sinks. Overall, this behavior could be explained by the permanently cold conditions, a dominant autotrophy over the annual cycle, and the low exogenous organic input received by the aquatic ecosystems (except OP2), as suggested by the absence of vegetation, and limited/absent anthropogenic and ornithogenic nutrient inputs. Compared to other freshwater ecosystems, previously reported in other regions of the maritime Antarctica, the CH<sub>4</sub> cycle indicators were lower but within the same magnitude order. Thus, we conclude that the non-perennially glaciated aquatic ecosystems located around the Antarctic continent probably do not contribute significantly to the greenhouse gas emissions associated to the aquatic ecosystems located at other latitudes. Moreover, in the context of future warming, with longer ice-free periods and larger ice-free areas in Antarctica, these lakes which could gain importance and may convert to a standard feature of the Antarctic landscape, are unlikely to modify substantially the current greenhouse gas budget.

## **CRedit authorship contribution statement**

Frederic Thalasso: Conceptualization, formal analysis, field investigation, data curation writing - original draft. Armando Sepulveda-Jauregui: field investigation, data processing, writing - original draft. Léa Cabrol: field investigation, data processing, writing - original draft. Céline Lavergne: field investigation, data processing, writing - original draft. Nazlı Olgun: field investigation, laboratory analysis. Karla Martinez-Cruz: laboratory analysis, data processing. Polette Aguilar-Muñoz: laboratory análisis, data processing. Natalia Calle: laboratory analysis, data processing. Andrés Mansilla: writing - review & editing. María Soledad Astorga-España: Conceptualization, funding acquisition, writing - review & editing.

## **Data availability**

Data will be made available on request.

## **Declaration of competing interest**

The authors declare that they have no known competing financial interests or personal relationships that could have appeared to influence the work reported in this paper.

## **Acknowledgement**

This project was financially supported by the “Instituto Antártico Chileno” (INACH, project RT\_14-15). This project was also partially funded by the Cape Horn International Center project (CHIC-FB210018). F. Thalasso received financial support from the “Consejo Nacional de Ciencia y Tecnología” (Conacyt, project #255704). N. Olgun was funded by Istanbul Technical University (ITU Project #40265).

## Appendix A. Supplementary data

Supplementary data to this article can be found online at <https://doi.org/10.1016/j.scitotenv.2022.157485>.

## References

- Aguilar-Muñoz, P., Lavergne, C., Chamy, R., Cabrol, L., 2022. The biotechnological potential of microbial communities from Antarctic soils and sediments: application to low temperature biogenic methane production. *J. Biotechnol.* 351, 38–49. <https://doi.org/10.1016/J.JBIOTECH.2022.04.014>.
- Ashmore, D.W., Bingham, R.G., 2014. Antarctic subglacial hydrology: current knowledge and future challenges. *Antarct. Sci.* 26, 758–773. <https://doi.org/10.1017/S0954102014000546>.
- Bañón, M., Justel, A., Velázquez, D., Quesada, A., 2013. Regional weather survey on byers peninsula, Livingston Island, South Shetland Islands, Antarctica. *Antarct. Sci.* 25, 146–156. <https://doi.org/10.1017/S0954102012001046>.
- Bastviken, D., Tranvik, L.J., Downing, J.A., Crill, P.M., Enrich-Prast, A., 2011. Freshwater methane emissions offset the continental carbon sink. *Science* 331. <https://doi.org/10.1126/science.1196808> 50–50.
- Beaulieu, J.J., Downing, J.A., 2019. Eutrophication will increase methane emissions from lakes and impoundments during the 21st century. *Nat. Commun.* 3–7. <https://doi.org/10.1038/s41467-019-09100-5>.
- Borrel, G., Jézéquel, D., Biderre-Petit, C., Morel-Desrosiers, N., Morel, J.P., Peyret, P., Fonty, G., Lehours, A.C., 2011. Production and consumption of methane in freshwater lake ecosystems. *Res. Microbiol.* 162, 833–847. <https://doi.org/10.1016/j.resmic.2011.06.004>.
- Burkins, M.B., Virginia, R.A., Chamberlain, C.P., Wall, D.H., 2000. Origin and distribution of soil organic matter in Taylor Valley, Antarctica. *Ecology* 81, 2377. <https://doi.org/10.2307/177461>.
- Burkins, M.B., Virginia, R.A., Wall, D.H., 2001. Organic carbon cycling in Taylor Valley, Antarctica: quantifying soil reservoirs and soil respiration. *Glob. Chang. Biol.* 7, 113–125. <https://doi.org/10.1046/j.1365-2486.2001.00393.x>.
- Cabrol, L., Thalasso, F., Gandois, L., Sepulveda-Jauregui, A., Martinez-Cruz, K., Teisserenc, R., Tananaev, N., Tveit, A., Svenning, M.M., Barret, M., 2020. Anaerobic oxidation of methane and associated microbiome in anoxic water of northwestern siberian lakes. *Sci. Total Environ.* 736, 139588. <https://doi.org/10.1016/j.scitotenv.2020.139588>.
- Campos, H., Arenas, J., Steffen, W., 1978. Antecedentes y observaciones limnológicas en los principales Lagos de la isla rey Jorge, shetland del Sur, Antártica. *Ser. Cient.* 24, 11–19.
- Cavichiolli, R., 2006. Cold-adapted archaea. *Nat. Rev. Microbiol.* 5 (4), 331–343. <https://doi.org/10.1038/nrmicro1390> 2006 4.
- Cohen, A.P., Melack, J.M., 2020. Carbon dioxide supersaturation in high-elevation oligotrophic lakes and reservoirs in the Sierra Nevada, California. *Limnol. Oceanogr.* 65, 612–626. <https://doi.org/10.1002/LNO.11330>.
- Cole, J.J., Prairie, Y.T., 2009. Dissolved CO<sub>2</sub>. *Encyclopedia of Inland Waters*, pp. 30–34. <https://doi.org/10.1016/B978-012370626-3.00091-0>.
- Conrad, R., 2020. Methane production in soil environments—anaerobic biogeochemistry and microbial life between flooding and desiccation. *Microorganisms* 8(8), 881. <https://doi.org/10.3390/MICROORGANISMS8080881>.
- Contreras, M., Cabrera, S., Montecino, V., Pizzarro, G., 1991. Dinámica abiótica de lago kitiesh, Antártica. *Ser. Cient.* 41, 9–32.
- Deemer, B.R., Hølgerson, M.A., 2021. Drivers of methane flux differ between lakes and reservoirs, complicating global upscaling efforts. *Geophys. Res. Biogeosci.* 126, e2019JG005600. <https://doi.org/10.1029/2019JG005600>.
- Delsontro, T., McGinnis, D.F., Wehrli, B., Ostrovsky, I., 2015. Size does matter: importance of large bubbles and small-scale hot spots for methane transport. *Environ. Sci. Technol.* 49 (3), 1268–1276. <https://doi.org/10.1021/es5054286>.
- DelSontro, T., Beaulieu, J.J., Downing, J.A., 2018. Greenhouse gas emissions from lakes and impoundments: upscaling in the face of global change. *Limnol. Oceanogr. Lett.* 3, 64–75. <https://doi.org/10.1002/LOL2.10073>.
- Diem, T., Koch, S., Schwarzenbach, S., Wehrli, B., Schubert, C.J., 2012. Greenhouse gas emissions (CO<sub>2</sub>, CH<sub>4</sub>, and N<sub>2</sub>O) from several perialpine and alpine hydropower reservoirs by diffusion and loss in turbines. *Aquat. Sci.* 74 (3), 619–635. <https://doi.org/10.1007/S00027-012-0256-5> 2012 74.
- Ding, W., Zhu, R., Ma, D., Xu, H., 2013. Summertime fluxes of N<sub>2</sub>O, CH<sub>4</sub> and CO<sub>2</sub> from the littoral zone of Lake daming, East Antarctica: effects of environmental conditions. *Antarct. Sci.* 25, 752–762. <https://doi.org/10.1017/S0954102013000242>.
- Dirección General De Aeronáutica Civil, 2022. <https://climatologia.meteochile.gob.cl/application/mensual/viento10DireccionesMensual/958130001/2017/1>. (Accessed 3 July 2022).
- Elberling, B., Gregorich, E.G., Hopkins, D.W., Sparrow, A.D., Novis, P., Greenfield, L.G., 2006. Distribution and dynamics of soil organic matter in an Antarctic dry valley. *Soil Biol. Biochem.* 38, 3095–3106. <https://doi.org/10.1016/J.SOILBIO.2005.12.011>.
- Ellis-Evans, J.C., 1984. Methane in maritime Antarctic freshwater lakes. *Polar Biol.* 3, 63–71. <https://doi.org/10.1007/BF00258149> 1984 3:2.
- Engel, F., Farrell, K.J., McCullough, I.M., Scordo, F., Denfeld, B.A., Dugan, H.A., de Eyto, E., Hanson, P.C., McClure, R.P., Nöges, P., Nöges, T., Ryder, E., Weathers, K.C., Weyhenmeyer, G.A., 2018. A lake classification concept for a more accurate global estimate of the dissolved inorganic carbon export from terrestrial ecosystems to inland waters. *Sci. Nat.* 105, 25. <https://doi.org/10.1007/s00114-018-1547-z>.
- Fuentes, N., Güde, H., Wessels, M., Straile, D., 2013. Allochthonous contribution to seasonal and spatial variability of organic matter sedimentation in a deep oligotrophic lake (Lake Constance). *Limnologia* 43, 122–130. <https://doi.org/10.1016/J.LIMNO.2012.06.003>.
- Garbe, J., Albrecht, T., Levermann, A., Donges, J.F., Winkelmann, R., 2020. The hysteresis of the Antarctic Ice Sheet. *Nature* 7826 (585), 538–544. <https://doi.org/10.1038/s41586-020-2727-5> 585.
- Gerardo-Nieto, O., Astorga-España, M.S., Mansilla, A., Thalasso, F., 2017. Initial report on methane and carbon dioxide emission dynamics from sub-Antarctic freshwater ecosystems: a seasonal study of a lake and a reservoir. *Sci. Total Environ.* 593–594, 144–154. <https://doi.org/10.1016/j.scitotenv.2017.02.144>.
- Gonzalez-Valencia, R., Magana-Rodriguez, F., Gerardo-Nieto, O., Sepulveda-Jauregui, A., Martinez-Cruz, K., Walter Anthony, K., Baer, D., Thalasso, F., 2014. In situ measurement of dissolved methane and carbon dioxide in freshwater ecosystems by off-Axis integrated cavity output spectroscopy. *Environ. Sci. Technol.* 48, 11421–11428. <https://doi.org/10.1021/es500987j>.
- Greene, S., Anthony, K.M.W., Archer, D., Sepulveda-Jauregui, A., Martinez-Cruz, K., 2014. Modeling the impediment of methane ebullition bubbles by seasonal lake ice modeling the impediment of methane ebullition bubbles by seasonal lake ice modeling the impediment of methane ebullition bubbles by seasonal lake ice. *Biogeosciences* 11, 6791–6811. <https://doi.org/10.5194/bg-11-6791-2014>.
- Gregorich, E.G., Hopkins, D.W., Elberling, B., Sparrow, A.D., Novis, P., Greenfield, L.G., Rochette, P., 2006. Emission of CO<sub>2</sub>, CH<sub>4</sub> and N<sub>2</sub>O from lakeshore soils in an Antarctic dry valley. *Soil Biol. Biochem.* 38, 3120–3129. <https://doi.org/10.1016/J.SOILBIO.2006.01.015>.
- Guggenheim, C., Brand, A., Bürgmann, H., Sigg, L., Wehrli, B., 2019. Aerobic methane oxidation under copper scarcity in a stratified lake. *Sci. Rep.* 1 (9), 1–11. <https://doi.org/10.1038/s41598-019-40642-9>.
- ISO, 1992. Spectrometric determination of the chlorophyll-a concentration. <https://www.iso.org/standard/18300.html>.
- Kling, G.W., Kipphut, G.W., Miller, C., 1992. The flux of CO<sub>2</sub> and CH<sub>4</sub> from lakes and rivers in arctic Alaska. *Hydrobiologia* 240, 23–36. <https://doi.org/10.1007/BF00013449>.
- Laas, A., Nöges, P., Köiv, T., Nöges, T., 2012. High-frequency metabolism study in a large and shallow temperate lake reveals seasonal switching between net autotrophy and net heterotrophy. *Hydrobiologia* 694, 57–74. <https://doi.org/10.1007/S10750-012-1131-z> 694:1.
- Larraín, J., Bahamonde, N., 2017. Los briófitos de la estancia cerro Paine, parque nacional Torres del Paine, magallanes, Chile. *Bol. Soc. Argent. Bot.* 52, 27–38. <https://doi.org/10.31055/1851.2372.V52.N1.16905>.
- Lavergne, C., Aguilar-Muñoz, P., Calle, N., Thalasso, F., Astorga-España, M.S., Sepulveda-Jauregui, A., Martinez-Cruz, K., Gandois, L., Mansilla, A., Chamy, R., Barret, M., Cabrol, L., 2021. Temperature differently affected methanogenic pathways and microbial communities in sub-Antarctic freshwater ecosystems. *Environ. Int.* 154, 106575. <https://doi.org/10.1016/J.ENVINT.2021.106575>.
- Lee, Y.I., Lim, H.S., Yoon, H.I., 2004. Geochemistry of soils of King George Island, South Shetland Islands, West Antarctica: implications for pedogenesis in cold polar regions. *Geochim. Cosmochim. Acta* 68, 4319–4333. <https://doi.org/10.1016/J.GCA.2004.01.020>.
- Li, W., Dore, J.E., Steigmeyer, A.J., Cho, Y.J., Kim, O.S., Liu, Y., Morgan-Kiss, R.M., Skidmore, M.L., Priscu, J.C., 2020. Methane production in the oxygenated water column of a perennially ice-covered Antarctic lake. *Limnol. Oceanogr.* 65, 143–156. <https://doi.org/10.1002/LNO.11257>.
- Liikanen, A., Huttunen, J.T., Valli, K., Martikainen, P.J., 2002. Methane cycling in the sediment and water column of mid-boreal hyper-eutrophic Lake Kevätön, Finland. *Fundam. Appl. Limnol.* 154, 585–603. <https://doi.org/10.1127/archiv-hydrobiol/154/2002/585>.
- Lofton, D.D., Whalen, S.C., Hershey, A.E., 2014. Effect of temperature on methane dynamics and evaluation of methane oxidation kinetics in shallow Arctic alaskan lakes. *Hydrobiologia* 721, 209–222. <https://doi.org/10.1007/s10750-013-1663-x>.
- López-Martínez, J., Serrano, E., Schmid, T., Mink, S., Linés, C., 2012. Periglacial processes and landforms in the South Shetland Islands (northern Antarctic peninsula region). *Geomorphology* 155–156, 62–79. <https://doi.org/10.1016/J.GEOMORPH.2011.12.018>.
- Martinez-Cruz, K., Sepulveda-Jauregui, A., Escobar-Orozco, N., Thalasso, F., 2012. Methanogenic activity tests by infrared tunable diode laser absorption spectroscopy. *J. Microbiol. Methods* 91 (1), 89–92. <https://doi.org/10.1016/j.mimet.2012.07.022>.
- Martinez-Cruz, K., Sepulveda-Jauregui, A., Walter Anthony, K., Thalasso, F., 2015. Geographic and seasonal variation of dissolved methane and aerobic methane oxidation in alaskan lakes. *Biogeosciences* 12, 4595–4606. <https://doi.org/10.5194/bg-12-4595-2015>.
- Martinez-Cruz, K., Sepulveda-Jauregui, A., Greene, S., Fuchs, A., Rodriguez, M., Pansch, N., Gonsiorczyk, T., Casper, P., 2020. Diel variation of CH<sub>4</sub> and CO<sub>2</sub> dynamics in two contrasting temperate lakes. *Inland Waters* 10, 333–347. <https://doi.org/10.1080/20442041.2020.1728178>.
- Myhre, G., Shindell, D., Breon, F.M., Collins, W., Fuglested, J., Huang, J., Koch, D., Lamarque, J.F., Lee, D., Mendoza, B., Nakajima, T., Robock, A., Stephens, G., Takemura, T., Zhang, H., 2013. Anthropogenic and natural radiative forcing. *Climate Change 2013: The Physical Science Basis, Contribution of Working Group I to the Fifth Assessment Report of the Intergovernmental Panel on Climate Change*. Cambridge University Press, Cambridge, United Kingdom and New York, NY, USA 1984 3:2.
- Neogonekdzarek, A., Pocięcha, A., 2010. Limnological characterization of freshwater systems of the Thomas point oasis (Admiralty Bay, King George Island, West Antarctica). *Polar Sci.* 4, 457–467. <https://doi.org/10.1016/J.POLAR.2010.05.008>.
- NIST, 2020. *National Institute of Standards and Technology Chemistry Web Book*, 2020.
- Obu, J., Westermann, S., Bartsch, A., Berdnikov, N., Christiansen, H.H., Dashtseren, A., Delaloye, R., Elberling, B., Etzelmüller, B., Kholodov, A., Khorutov, A., Kääh, A., Leibman, M.O., Lewkowicz, A.G., Panda, S.K., Romanovsky, V., Way, R.G., Westergaard-Nielsen, A., Wu, T., Yamkhin, J., Zou, D., 2019. Northern hemisphere permafrost map based on TTOP modelling for 2000–2016 at 1 km<sup>2</sup> scale. *Earth Sci. Rev.* 193, 299–316. <https://doi.org/10.1016/J.EARSCIREV.2019.04.023>.
- Peeters, F., Encinas Fernandez, J., Hofmann, H., 2019. Sediment fluxes rather than oxic methanogenesis explain diffusive CH<sub>4</sub> emissions from lakes and reservoirs. *Sci. Rep.* 9, 243. <https://doi.org/10.1038/s41598-018-36530-w>.

- Pighini, S., Ventura, M., Miglietta, F., Wohlfahrt, G., 2018. Dissolved greenhouse gas concentrations in 40 lakes in the alpine area. *Aquat. Sci.* 80, 32. <https://doi.org/10.1007/s00027-018-0583-2>.
- Pirk, N., Mastepanov, M., Parmentier, F.W., Lund, M., Crill, P., 2016. Calculations of automatic chamber flux measurements of methane and carbon dioxide using short time series of concentrations. *Biogeosciences* 903–912. <https://doi.org/10.5194/bg-13-903-2016>.
- R Core Team, 2022. R: A language and environment for statistical computing. Version Software 4.0.4R Foundation for Statistical Computing, Vienna, Austria. <https://www.R-project.org/>.
- Ragg, R.B., Peeters, F., Ingwersen, J., Teiber-Siessegger, P., Hofmann, H., 2021. Interannual variability of methane storage and emission during autumn overturn in a small lake. *J. Geophys. Res. Biogeosci.* 126, e2021JG006388. <https://doi.org/10.1029/2021JG006388>.
- Raymond, P.A., Hartmann, J., Lauerwald, R., Sobek, S., McDonald, C., Hoover, M., Butman, D., Striegl, R., Mayorga, E., Humborg, C., Kortelainen, P., Dürr, H., Meybeck, M., Ciais, P., Guth, P., 2013. Global carbon dioxide emissions from inland waters. *Nature* 503, 355–359. <https://doi.org/10.1038/nature12760>.
- Roldán, D.M., Carrizo, D., Sánchez-García, L., Menes, R.J., 2022. Diversity and effect of increasing temperature on the activity of methanotrophs in sediments of Fildes Peninsula Freshwater Lakes, King George Island, Antarctica. *Front. Microbiol.* 13. <https://doi.org/10.3389/fmicb.2022.822552>.
- Samad, M.S., Bertilsson, S., 2017. Seasonal variation in abundance and diversity of bacterial methanotrophs in five temperate lakes. *Front. Microbiol.* 8, 142. <https://doi.org/10.3389/fmicb.2017.00142/BIBTEX>.
- Sasaki, M., Imura, S., Kudoh, S., Yamanouchi, T., Morimoto, S., Hashida, G., 2009. Methane efflux from bubbles suspended in ice-covered lakes in syowa oasis, East Antarctica. *J. Geophys. Res. Atmos.* 114, 18114. <https://doi.org/10.1029/2009JD011849>.
- Sasaki, M., Endoh, N., Imura, S., Kudoh, S., Yamanouchi, T., Morimoto, S., Hashida, G., 2010. Air-lake exchange of methane during the open water season in syowa oasis, East Antarctica. *J. Geophys. Res. Atmos.* 115, 16313. <https://doi.org/10.1029/2010JD013822>.
- Saunio, M., Stavert, A., Poulter, B., Bousquet, P., Canadell, J., Jackson, R., Raymond, P., Dlugokencky, E., Houweling, S., Patra, P., Ciais, P., Arora, V., Bastviken, D., Bergamaschi, P., Blake, D., Brailsford, G., Bruhwiler, L., Carlson, K., Carrol, M., Castaldi, S., Chandra, N., Crevoisier, C., Crill, P., Covey, K., Curry, C., Etiope, G., Frankenberg, C., Gedney, N., Hegglin, M., Höglund-Isaksson, L., Hugelius, G., Ishizawa, M., Ito, A., Janssens-Maenhout, G., Jensen, K., Joos, F., Kleinen, T., Krümmel, P., Langenfelds, R., Laruelle, G., Liu, L., Machida, T., Maksyutov, S., McDonald, K., McNorton, J., Miller, P., Melton, J., Morino, I., Müller, J., Murguía-Flores, F., Naik, V., Niwa, Y., Noce, S., O'Doherty, S., Parker, R., Peng, C., Peng, S., Peters, G., Prigent, C., Prinn, R., Ramonet, M., Regnier, P., Riley, W., Rosentretter, J., Segers, A., Simpson, I., Shi, H., Smith, S., Steele, L.P., Thornton, B., Tian, H., Tohjima, Y., Tubiello, F., Tsuruta, A., Viovy, N., Voulgarakis, A., Weber, T., van Weele, M., van der Werf, G., Weiss, R., Worthy, D., Wunch, D., Yin, Y., Yoshida, Y., Zhang, W., Zhang, Z., Zhao, Y., Zheng, B., Zhu, Q., Qing, Zhu, Q., 2020. The global methane budget 2000–2017. *Earth Syst. Sci. Data* 12, 1561–1623. <https://doi.org/10.5194/essd-12-1561-2020>.
- Serikova, S., Pokrovsky, O.S., Laudon, H., Krickov, I.V., Lim, A.G., Manasypov, R.M., Karlsson, J., 2019. High carbon emissions from thermokarst lakes of Western Siberia. *Nat. Commun.* 10. <https://doi.org/10.1038/s41467-019-09592-1>.
- Sun, L., Zhu, R., Xie, Z., Xing, G., 2002. Emissions of nitrous oxide and methane from Antarctic tundra: role of penguin dropping deposition. *Atmos. Environ.* 36, 4977–4982. [https://doi.org/10.1016/S1352-2310\(02\)00340-0](https://doi.org/10.1016/S1352-2310(02)00340-0).
- Unrein, F., 2000. Estructura y dinámica del fitoplancton estival de un lago antártico (Península potter, shetland del Sur). *Ecol. Austral* 10, 169–179.
- Verpoorter, C., Kutser, T., Seekell, D.A., Tranvik, L.J., 2014. A global inventory of lakes based on high-resolution satellite imagery. *Geophys. Res. Lett.* 41, 6396–6402. <https://doi.org/10.1002/2014GL060641>.
- Walter Anthony, K.M., Vas, D.A., Brosius, L., Stuart Chapin, I., Zimov, S.A., Zhuang, Q., 2010. Estimating methane emissions from northern lakes using ice-bubble surveys. *Limnol. Oceanogr. Methods* 8, 592–609. <https://doi.org/10.4319/LOM.2010.8.0592>.
- Walter, K.M., Zimov, S.A., Chanton, J.P., Verbyla, D., Iii, F.S.C., 2006. Methane Bubbling From Siberian Thaw Lakes as a Positive Feedback to Climate Warming. 443, pp. 71–75. <https://doi.org/10.1038/nature05040>.
- Wand, U., Samarkin, V.A., Nitzsche, H.-M., Hubberten, H.-W., Babenzien, H.-D., Casper, P., Conrad, R., Ellis-Evans, J.C., Heyer, J., Joye, S.B., Orcutt, B.N., 2006. Biogeochemistry of methane in the permanently ice-covered Lake Untersee, central Dronning Maud Land, East Antarctica. *Limnol. Oceanogr.* 51, 1180–1194. <https://doi.org/10.4319/LO.2006.51.2.1180>.
- West, W.E., Creamer, K.P., Jones, S.E., 2016. Productivity and depth regulate lake contributions to atmospheric methane. *Limnol. Oceanogr.* 61, S51–S61. <https://doi.org/10.1002/lno.10247>.
- Wetzel, R.G., 2001. *Limnology lake and river ecosystems. Low Temperature Physics*, 3rd ed Academic Press.
- Wik, M., Thornton, B.F., Bastviken, D., Uhlbäck, J., Crill, P.M., 2016. Biased sampling of methane release from northern lakes: a problem for extrapolation. *Geophys. Res. Lett.* 43, 1256–1262. <https://doi.org/10.1002/2015GL066501>.
- Willmott, C.J., Matsuura, K., 2007. On the use of dimensioned measures of error to evaluate the performance of spatial interpolators. *Int. J. Geogr. Inf. Sci.* 20, 89–102. <https://doi.org/10.1080/13658810500286976>.
- Woolway, R.L., Kraemer, B.M., Lenters, J.D., Merchant, C.J., O'Reilly, C.M., Sharma, S., 2020. Global lake responses to climate change. *Nat. Rev. Earth Environ.* 8 (1), 388–403. <https://doi.org/10.1038/s43017-020-0067-5>.
- Yvon-Durocher, G., Allen, A.P., Bastviken, D., Conrad, R., Gudas, C., St-Pierre, A., Thanh-Duc, N., del Giorgio, P.A., 2014. Methane fluxes show consistent temperature dependence across microbial to ecosystem scales. *Nature* 507, 488–491. <https://doi.org/10.1038/nature13164>.
- Zhu, R., Liu, Y., Ma, E., Sun, J., Xu, H., Sun, L., 2009. Nutrient compositions and potential greenhouse gas production in penguin guano, ornithogenic soils and seal colony soils in coastal Antarctica. *Antarct. Sci.* 21, 427–438. <https://doi.org/10.1017/S0954102009990204>.
- Zhu, R., Liu, Y., Xu, H., Huang, T., Sun, J., Ma, E., Sun, L., 2010. Carbon dioxide and methane fluxes in the littoral zones of two lakes, East Antarctica. *Atmos. Environ.* 44, 304–311. <https://doi.org/10.1016/j.atmosenv.2009.10.038>.

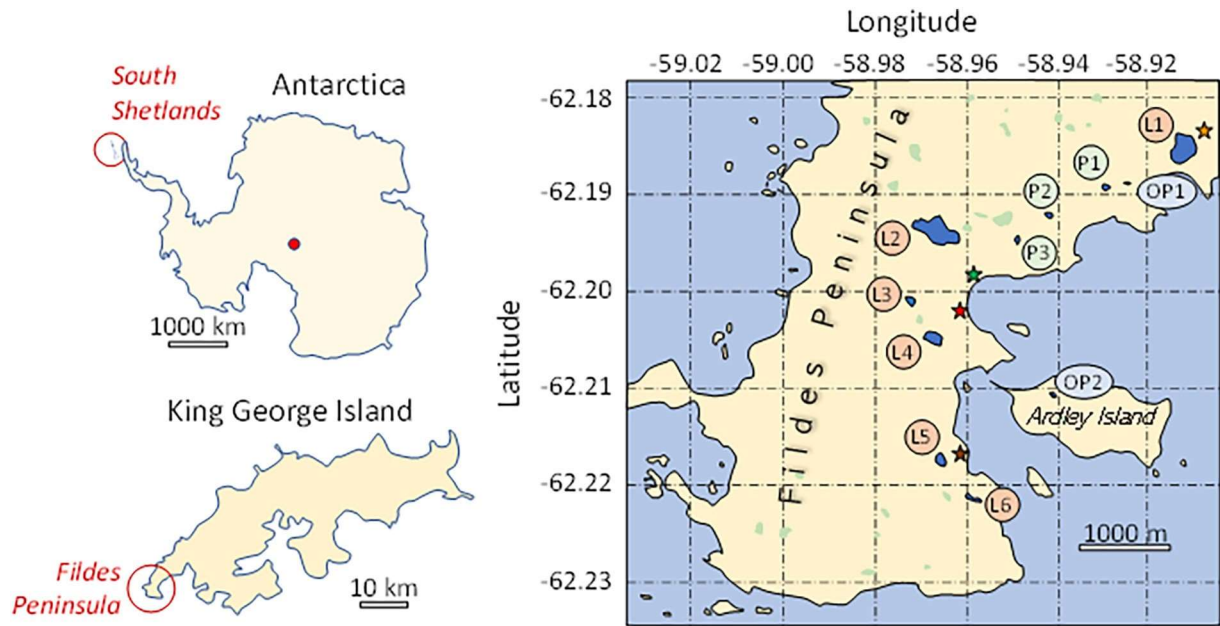


Fig. 1. Lakes (L), ponds (P) and organic ponds (OP) location in the Fildes Peninsula and Ardley Island, south of King George Island. Green areas represent other water bodies (not studied), stars represent scientific bases (★ Uruguay, ★ Russia, ★ Chile, ★ China).

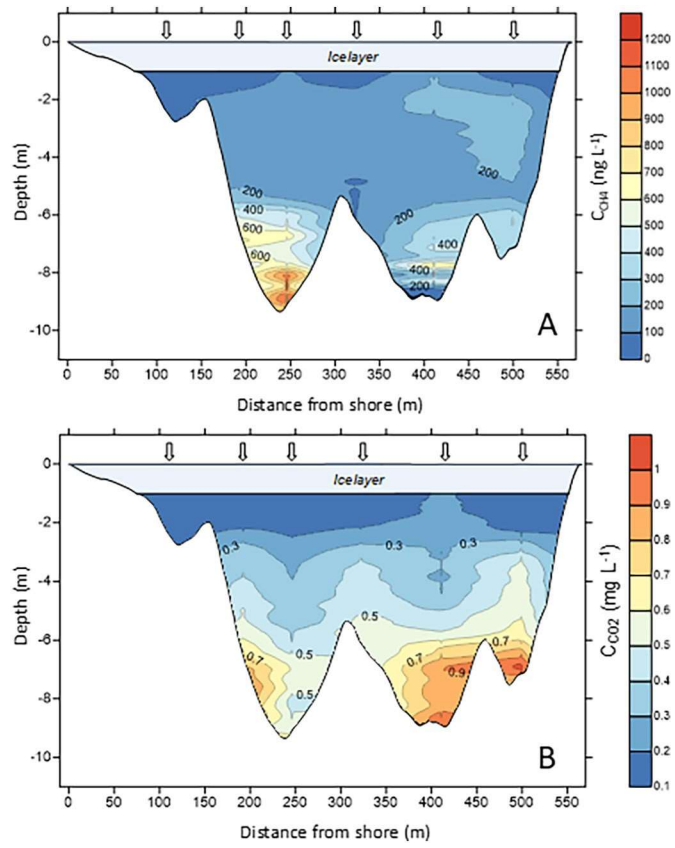


Fig. 2. East-West transect dissolved concentration of  $CH_4$  (A) and  $CO_2$  (B) during the ice-season in lake Kitiash (L2). White vertical arrows indicate the location of the profiles done with the M-ICOS method. Note the different magnitude of units in each panel.



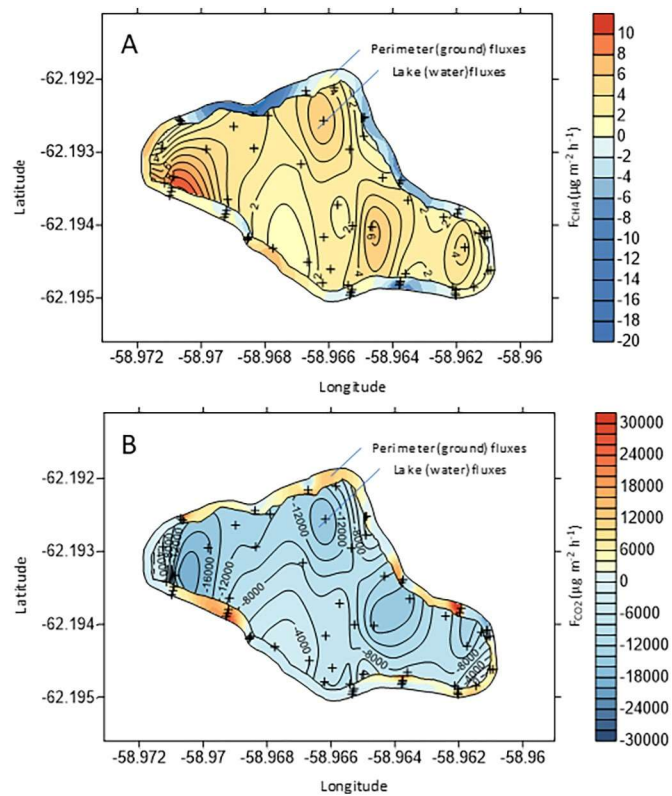


Fig. 3. CH<sub>4</sub> (A) and CO<sub>2</sub> (B) fluxes of lake Kitiesh (L2) and its surrounding ecosystem, observed during the ice-free season. Note the different magnitude of units in each panel.

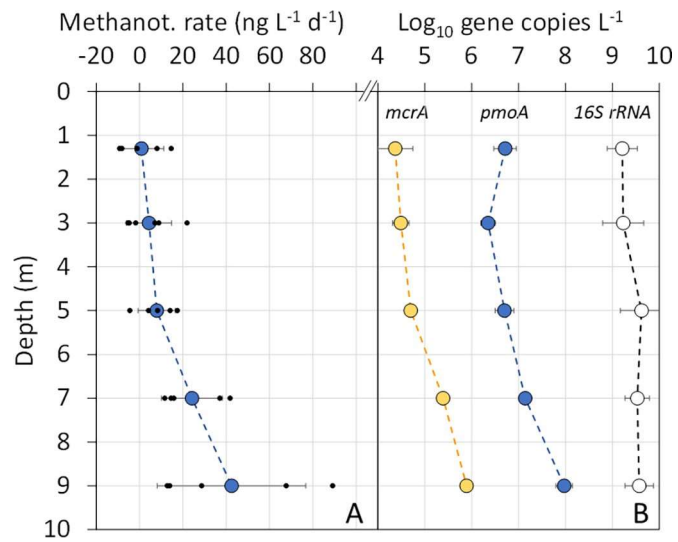


Fig. 4. (A) Methanotrophic rates and (B) gene copy number observed in the watercolumn of lake Kitiash (L2) during the ice-season. Each point represents the mean of four replicates and standard deviations are shown. *mcrA* and *pmoA* genes are marker genes of methanogens and methanotrophs, respectively. Note that the 16SrRNA gene copy number corresponds to the sum of both bacterial and archaeal 16S rRNA gene copies, representing all prokaryotes (Table S2).